Chapter 8
Crystallization

Nicolas Verhoeven, Tze Loon Neoh, Takeshi Furuta and Hidefumi Yoshii

Abstract Ethanol-mediated crystal transformation is a promising method for obtaining stable anhydrous crystals with a porous structure. The DSC (Differential scanning calorimetry)-coupled ethanol method was used to obtain anhydrous trehalose crystals with a specific size and shape by controlling the water content of the ethanol. DSC analysis of the crystal transformation reaction of trehalose or maltose under isothermal and non-isothermal conditions allowed an overall evaluation of the activation energy of crystal transformation, and presumably revealed two different transformation reactions in the glassy state before the click point temperatures and the rubbery state after the click point temperatures. Anhydrous sugar crystals with an increased specific surface area were produced via ethanol-mediated crystal transformation under appropriate conditions. These porous crystals with high surface area could be applied to encapsulate flavor or functional foods. Thin needle-shaped sugar crystals can also be used to form a creamy, non-oil gel in over supersaturated solution conditions.

Keywords Trehalose · Sugar · Ethanol · Dehydration anhydrous · Hydrous · Crystal transformation

8.1 Introduction

Sugars are among the most important major components in food. Sugars come naturally in their hydrous forms. This study includes (1) the concept and molecular arrangement of hydrous crystal sugar or amorphous solid to the formation of anhydrous crystal sugar, and (2) the concept of physical property changes and

N. Verhoeven · T. Furuta
Department of Biotechnology, Tottori University, Koyama Minami 4-101, Tottori 680-8552, Japan

T.L. Neoh · H. Yoshii (✉)
Department of Applied Biological Science, Kagawa University, 2393 Ikenobe, Miki-Cho, Kita, Kagawa 761-0795, Japan
e-mail: foodeng.yoshii@ag.kagawa-u.ac.jp

Y.H. Roos and Y.D. Livney (eds.), *Engineering Foods for Bioactives Stability and Delivery*, Food Engineering Series,
DOI 10.1007/978-1-4939-6595-3_8

molecular mobility around the glass transition, as well as mathematical descriptions of crystal transformation and influences on food stability.

Diffusion of water in foods is important in product development, processing, and storage design. The rate of crystal structure changes often depends on the physical state and, therefore, on temperature and water content.

Crystal forms are very useful in the food industry for storing sugar or salt food additives. Hartel and Shastry (1991) reviewed sugar crystallization in food products, with an emphasis on the relationship between these crystallization phenomena and the solution structure for comparison purposes. The effects of fat crystals in food emulsion formation and stability are reviewed by Rousseau (2000). During processing and/or storage, intraglobular fat (e.g. in cream) may solidify, forming crystals that can protrude through the interface, leading to droplet coalescence (Boode et al. 1991). There are several papers on fat crystal and water-in-oil emulsion stability (Supratim and Rousseau 2011), but little is known about the crystal transformation of sugars. Crystalline sugars typically exist in anhydrate and hydrated forms, such as lactose and lactose monohydrate, glucose and glucose monohydrate, maltose and maltose monohydrate, trehalose and trehalose dihydrates, α-, β-, and γ-cyclodextrins (CDs), and hexa-, dodeca-, and higher hydrates (Nakai et al. 1986). It is well known that hydrous and anhydrous forms are usually present as forms of crystalline saccharides and that hydrous crystals can be converted into anhydrous crystals, and vice versa. The forms are mutually converted through a dehydration process performed by heating (drying method) and moisture absorption. Saccharides can be effectively used on an industrial scale by using those characteristics of converting the forms between hydrous and anhydrous crystal.

Carbohydrates have a wide range of applications in a variety of industries (textiles, plastics, food, pharmaceuticals, etc.) and are also used in biological applications. For example, lactose is commonly used as filler in pharmaceutical capsule and tablet formulations and as a carrier in dry powder inhalation devices (Chidavaenzi et al. 1997; Buckton et al. 2002). It is also commonly applied as an ingredient in dairy-based food products such as infant formula. The α-monohydrate is typically used in wet granulation formulations, while the β-anhydrous phase is used as a direct compression ingredient. For direct tableting, different forms of agglomerated lactose, such as spray-dried lactose, are used. The drying step in the manufacturing of spray-dried α-monohydrate is a very sensitive operation because of the possibility of physical modifications of lactose occurring during the drying process (Vromans et al. 1987).

This chapter investigates crystal transformation characteristics from the hydrate to the anhydrate via solvent-mediated transformation, in order to produce new crystalline material with an improved specific surface area. The kinetics and mechanism of the crystal transformation are discussed, as well as the influence on the crystal structure and possible applications.

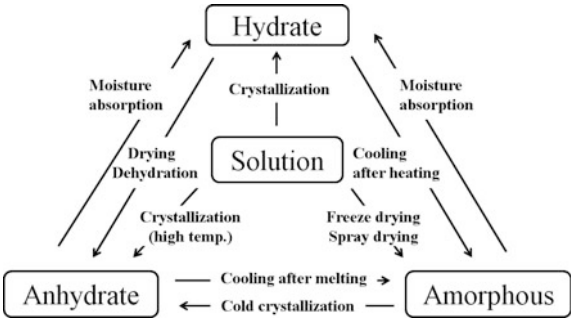

Fig. 8.1 Phase transitions of sugars

8.2 Phase Transitions of Carbohydrates

A phase transition is the transformation of a thermodynamic system from one phase or state of matter to another. The phases of a thermodynamic system and the states of matter have uniform physical properties. In the case of sugars, the possible phase transitions are summarized in Fig. 8.1. Starkting from a sugar solution, either the hydrate or the anhydrate crystalline forms can be obtained by crystallization under appropriate conditions. The anhydrate formation is typically favored by high-temperature conditions (Roos and Karel 1992; Figura and Epple 1995; Jones et al. 2006). The amorphous (i.e. non-crystalline form) phase can be produced by processes such as grinding (Lappalainen et al. 2006), freeze drying (Gabarra and Hartel 1998; Kedward et al. 1998; Gloria and Sievert 2001; Mazzobre et al. 2001), spray drying (Aguilar et al. 1994; Sussich and Cesàro 2008), lyophilization (Van Scoik and Carstensen 1990), by cooling after melting (Sussich et al. 2002), or dehydration and melt quenching (Surana et al. 2004; Simperler et al. 2006). The hydrate form is also produced from either the anhydrate or the amorphous phase by moisture absorption under mild or high relative humidity conditions (Crowe et al. 1996; Arvanitoyanis and Blanshard 1994; Kedward et al. 2000). The anhydrate phase can sometimes be obtained from the amorphous phase by cold crystallization (Saleki-Gerhardt and Zografi 1994) or by vacuum drying (O'Brien 1996). Note that the stability of the anhydrate crystal is an important parameter, which is studied in this dissertation. Finally, the transformation from hydrate to anhydrate is called dehydration (Jones et al. 2008; Kilburn and Sokol 2009). It is literally the removal of water from the hydrate to form the anhydrate.

8.3 "Soft" Dehydration and "Hard" Dehydration

Carbohydrate materials, especially mono- and disaccharides and products in which these are the main components such as fruit juices, are difficult to dry because of their sensitivity to temperature and water. In the food industry, it is the usual

procedure to detect and to use the most stable structure that consequently has the lowest solubility and the lowest free energy. Unfortunately, this is inconsistent with the demand for high dissolution rates because the phase with the lowest solubility in a certain solvent usually has the lowest dissolution rate.

In order to improve the dissolution rates, it is often necessary to lower the stability or to modify other physical properties of the compound. One of these physical properties is the shape of the crystals. Needle-like crystals lead to a significant increase in the specific surface area, thus improving the dissolution behavior and chemical reactions. Such an increase can be achieved by suspending crystalline substances in a solvent that induces phase transformations (Nordhoff and Ulrich 1999). In order to find new structures of several crystalline compounds, the methodology presented and applied in this chapter is devoted to the dehydration mechanism of molecular crystals and uses the existence of hydrates to promote the formation of new molecular packings by means of suitable dehydration conditions.

The simplified representation presented in Fig. 8.2 illustrates the fact that, starting from a hydrated structure, the use of hard dehydration conditions (such as high-temperature drying) is likely to produce an amorphous material, which can in turn evolve towards an anhydrous variety by means of a nucleation and growth mechanism. On the contrary, soft dehydration conditions (such as solvent-mediated crystal transformation) usually lead to a cooperative departure of water molecules, followed by a structural reorganization step leading to the nearest possible crystalline packing. This type of mechanism is, therefore, characterized by the persistence during the dehydration process of similar molecular contacts in the whole sample, in connection with the occurrence of continuous and cooperative molecular movements.

Moreover, the resulting packing is, at least to a certain extent, determined by the initial hydrated structure, so a part of the structural information is preserved, whereas the critical step for destructive–reconstructive mechanisms is likely to be the nucleation of the anhydrous variety, and the structural information is lost during such processes.

8.4 Solvent-Mediated Crystal Transformation Applied to Sugars

Trehalose, the disaccharide of α-D-glucose, is a naturally occurring sugar thought to confer anhydrobiotic properties (the ability to survive desiccation for long periods of time and rapidly resume metabolism upon rehydration) on various organisms in which it is found (Sussich et al. 2001, 2010). Trehalose shows polymorphism (Akao et al. 2001). In addition to the dihydrate, at least two anhydrous forms can be produced (Pinto et al. 2006). The anhydrous β-form can be formed from trehalose dihydrate by heating at 130 °C for 4 h (Reisener et al. 1962) or heating in a calorimeter under highly humid conditions, when it forms at 90 °C (Furuki et al. 2006). The anhydrous α-form is produced from the dihydrate by a slow thermal dehydration or supercritical CO_2 fluid extraction of the crystallization water

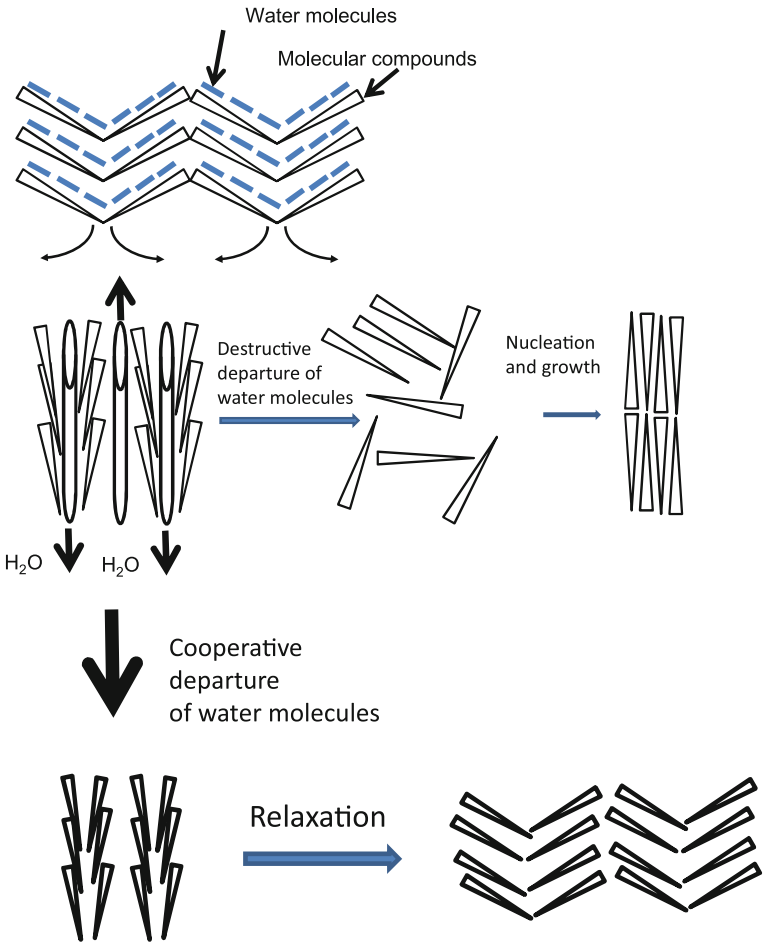

Fig. 8.2 Simplified representation of the methodology allowing the research of new polymorphic forms on the basis of different dehydration mechanisms (Garnier et al. 2002)

(Nagase et al. 2003; Willart et al. 2003). This anhydrous α-form can also be produced by dehydrating trehalose dihydrate at low relative humidity (0.1 % RH) and ambient temperature (25 °C) (Jones et al. 2006).

However, during these transformations, no drastic changes have been reported on the crystal structure.

Ohashi et al. (2007) investigated the crystal transformation of dihydrate trehalose to anhydrous trehalose using ethanol, and a new type of crystal particle with porous structure was obtained. The specific surface area of the anhydrous crystal transformed at 50 °C was 3.3 m^2/g, which was 5–8 times greater than that for anhydrous trehalose produced by vacuum drying and, for comparison, about 6 times higher than spray-dried α-lactose monohydrate (Cal et al. 1996) and 4–6

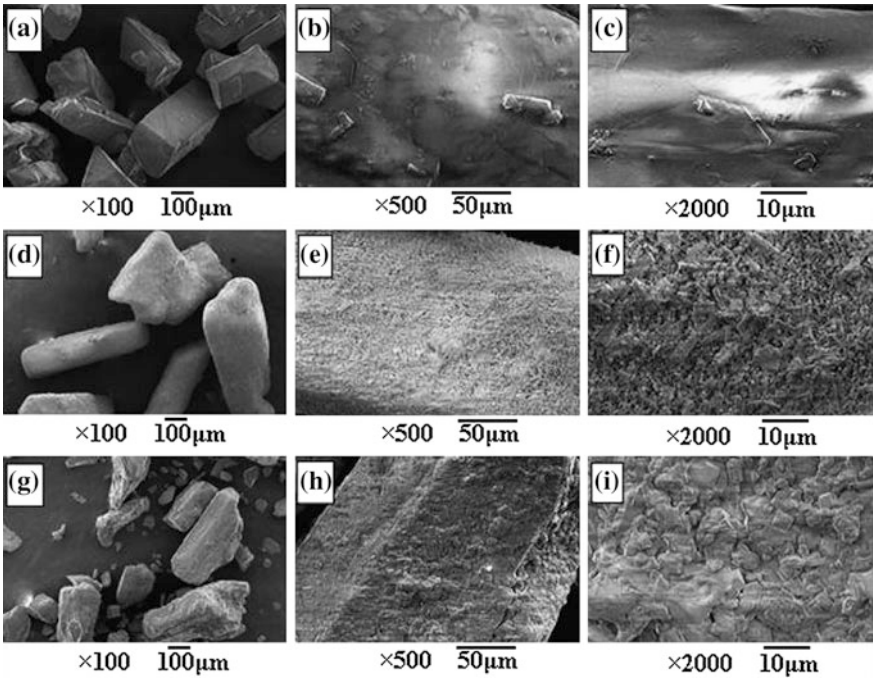

Fig. 8.3 SEM photomicrographs of anhydrous trehalose: **a–c** dihydrate crystal from solution, **a** ×100, **b** ×500, **c** ×2000, **d–f** anhydrous crystal transformed by the ethanol method, **d** ×100, **e** ×500, **f** ×2000, **g–i** anhydrous crystal transformed by vacuum drying, **g** ×100, **h** ×500, and **i** ×2000 (Ohashi et al. 2007)

times higher than some lactose excipients (Pitchayajittipong et al. 2010). The ethanol-mediated crystal transformation was performed in a glass reactor equipped with an agitation system. The porous structure of the anhydrous trehalose is shown in Fig. 8.3.

Garnier et al. (2002) observed the formation of whisker-like crystals during the dehydration of α-lactose monohydrate to anhydrous α-lactose in methanol or anhydrous β-lactose in acetone. Crystalline α-lactose monohydrate was obtained by Parrish and Brown (1982) from aqueous methanol or acetone solutions. The authors highlighted that the transformations were solid-state reactions, and not dissolution followed by recrystallization. In a recent work by Ohashi et al. (2009), α-cyclodextrin (α-CD) hexahydrate was transformed by the ethanol method, and porous crystalline ethanol dihydrate was obtained. The pore volume measured was 0.25 mL/g and the median pore diameter was 0.11 μm. The dissolution rate of this crystal was several times higher than that of (α-CD) hexahydrate or anhydrate obtained by drying.

8.5 Kinetics of Solvent-Mediated Crystal Transformation

For isothermal crystal transformation, the crystallization kinetics of many crystalline materials can be analyzed by the Avrami equation, which is generally written as:

$$x_c(t) = 1 - \exp(-(kt)^n) \tag{8.1}$$

In this equation, $x_c(t)$ is the normalized crystalline content at time t, and k and n are Avrami constants and are indicative of crystallization mechanisms that are involved. The exponent n in can provide information on nucleation type and crystal growth geometry. k is dependent upon the shape of the growing crystalline entities (e.g. whether they are spheres, discs, or rods), as well as the type and amount of nucleation (sporadic or predetermined). Basically, k is dependent on the reaction temperature, T_c, which affects the nucleation and growth rate. This equation is also called the Weibull distribution function, which has been successfully applied to describe shelf-life failure. A general empirical equation described by Weibull (1951) could be adapted to the dissolution/release process. This Avrami equation is essentially analogous to the equation of Kohlraush-Willian-Watt (KWW) (Alie 2004). Taking the logarithm of both sides of Eq. (8.1), we can get the parameter n as slope by plotting $\ln[-\ln(x_c)]$ versus $\ln t$ and release rate constant k from the interception at $\ln t = 0$. For n value, $n = 1$ represents the first-order reaction, and $n = 0.54$ represents the diffusion-limiting reaction kinetics. Table 8.1 shows the proposed equation for various solid reaction n values by Hancock and Sharp (1972). The derivation of the original model equation for solid reaction can be checked in the review by Hulbert (1969). Flavor release rates are strongly affected by the environmental humidity and temperature.

Figure 8.4 shows a typical endothermic peak of crystal transformation from hydrous sugar to its anhydrous form obtained from the isothermal measurement.

At constant temperature, the conversion fraction, $x(t)$, of the crystal transformation at time t is defined as:

$$x(t) = \frac{F(t)}{F(t_e)} \tag{8.2}$$

Table 8.1 Comparison of release mechanism n values using the model in the Avrami equation

Value of n	Release mechanism	Model equation
0.54	Diffusion-controlled (sphere)	$\left[1 - R^{1/3}\right]^2 = kt$
0.57	Diffusion-controlled (cylinder)	$R\ln R + 1 - R = kt$
0.62	Diffusion-controlled (tablet)	$(1 - R)^2 = kt$
1.00	First-order mechanism	$-\ln R = kt$
1.07	Moving interface mechanism (sphere)	$1 - R^{1/3} = kt$
1.11	Moving interface mechanism (disk)	$1 - R^{1/2} = kt$
1.24	Zero-order mechanism	$1 - R = kt$

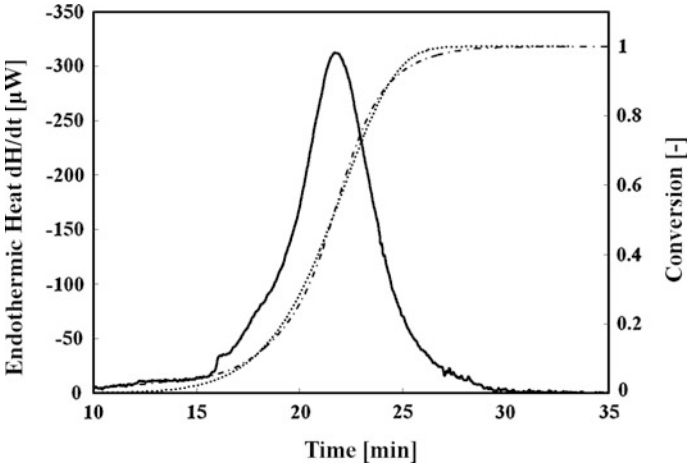

Fig. 8.4 DSC thermogram for crystal transformation from dihydrate trehalose to anhydrous trehalose under the isothermal conditions at 70 °C in ethanol with 2.5 % water content. *Solid line* Endothermic peak of crystal transformation; *Dashed line* conversion of the transformed material (using Simpson's rule); *Dotted line* conversion of the transformed material calculated with the Avrami equation for $n = 10$

where $F(t)$, as given by Eq. (8.2), is the integration of the DSC curve between the onset time of the crystal transformation reaction t_0 and an arbitrary time t before complete transformation is achieved at t_e, and $F(t_e)$ is the integration between t_0 and t_e, corresponding to the complete transformation.

$$F(t) = \int_{t_0}^{t} \left(-\frac{\mathrm{d}H}{\mathrm{d}t} \right) \mathrm{d}t \tag{8.3}$$

The term H represents the enthalpy of crystal transformation. The integration of Eq. (8.3) was approximated by numerical integration using Simpson's rule. The great number of data points makes this approximation highly accurate. For isothermal crystal transformation, the crystallization kinetics of many crystalline materials can be analyzed by the Avrami Eq. (8.1) (Avrami 1939, 1940).

For each T_c, the parameter n was fixed at 10, and the value of k that fitted best to the experimental data was calculated using Microsoft Excel Solver (dotted line in Fig. 8.4). The activation energy of the reactions was then approximated by the Arrhenius equation:

$$k = A \exp\left(-\frac{E_i}{RT_c} \right) \tag{8.4}$$

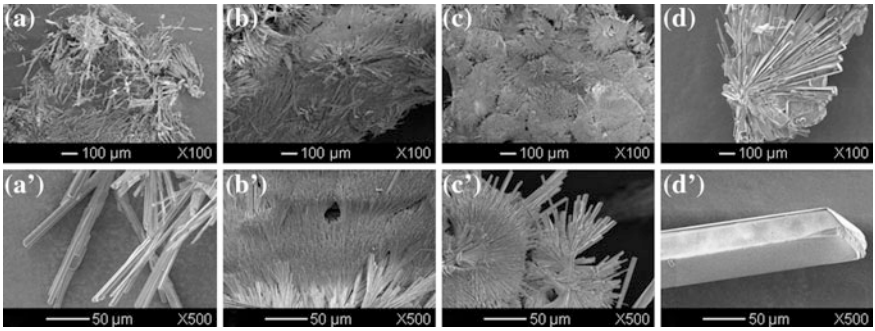

Fig. 8.5 Morphology of the anhydrous crystals obtained after a 30-min reaction at 70 °C with ethanol of **a**, **a′** 0.005, **b**, **b′** 0.4, **c**, **c′** 2.5, **d**, **d′** 4.0 % water content. The microscopy was performed at ×100 (**a**–**d**) and ×500 magnification (**a′**–**d′**)

where A is the frequency factor, E_i is the activation energy in J/mol, R is the gas constant (8.314 J/mol·K), and T_c is the reaction temperature in K. The activation energy was determined experimentally by carrying out the reaction at different reaction temperatures T_c.

8.6 Trehalose

Trehalose is a natural, non-reducing sugar formed from two glucose units joined by a 1-1 alpha bond, giving it the name of α-D-glucopyranosyl-(1 → 1)-α-D-glucopyranoside. Trehalose can be synthesized by fungi, plants, and invertebrate animals. It is implicated in anhydrobiosis, the ability of plants and animals to withstand prolonged periods of desiccation. It has high water retention capabilities and is used in food and cosmetics (Higashiyama 2002; Teramoto et al. 2008). There are two dominant theories as to how trehalose works within an organism in a state of cryptobiosis. They are the verification theory (Sussich et al. 2001), a state that prevents ice formation, and the water displacement theory (Crowe 1971), whereby water is replaced by trehalose, although it is possible that a combination of the two theories are at work (Sola-Penna and Meyer-Fernandes 1998). The only hydrous form of trehalose is dihydrate trehalose, but there are several anhydrous forms of trehalose. The first is known as the β-form and shows a characteristic melting point at 215 °C. The second is the α-form. Thermograms for this anhydrous α-form display a first endothermic peak at 125 °C and a melting slightly above 215 °C. The third anhydrous form, γ, is not stable, and can be distinguished from the α-form by the method of preparation, the enthalpy of melting, and the X-ray diffraction patterns (Sussich et al. 1998). Ohashi et al. (2008) investigated the encapsulation of flax seed oil in anhydrous crystalline maltose and trehalose with porous structure. Porous crystalline trehalose could be used as the matrix to encapsulate functional compounds. However, there are few investigations about the formation of anhydrous trehalose with porous structure by using solvent dehydration.

In the present study, the dehydration of trehalose in ethanol was performed in a differential scanning calorimeter in a high pressure crucible pan filled with ethanol.

Figure 8.5 shows the morphology of the anhydrous trehalose crystals obtained with ethanol of different water content after a 30 min transformation at 70 °C (isothermal conditions). The crystal size is highly dependent on the water content of the ethanol used. The crystals obtained with ethanol of 0.005 and 0.4 % water content had similar size and shape, with an average diameter of about 3 μm and an average length of 100 μm (Fig. 8.5a, b). When the water content in ethanol increased to 2.5 %, the size of the acicular crystals also increased, reaching an average diameter and length of 6 and 150 μm, respectively (Fig. 8.5c). At 4.0 % water content, the size of the acicular crystals greatly increased, achieving an average diameter and length of up to 50 and 500 μm, respectively (Fig. 8.5d).

Figure 8.6 shows the crystal transformation behavior from the initial dihydrate crystals to the anhydrous form. The dihydrate trehalose crystals surface is smooth and no porosity is observed (Fig. 8.6a). After 20 min of reaction at 70 °C in the ethanol of 0.005 % water content, cracks were observed on the surface of the crystals (Fig. 8.6b). At 25 min, slender acicular crystals were forming presumably from the surface to the core of the initial dihydrate crystal (Fig. 8.6c, d). These crystals are agglomerated in an acicular arrangement. Each needle has a diameter between 1 and 9 μm and an average length around 100 μm. The length-to-diameter ratio was over 10. The acicular crystals adopted a radial orientation. In these experiments, the anhydrous crystals obtained with the ethanol method were on average 10 times smaller than the dihydrate crystals. The needle-like crystal form can be attributed to the high local supersaturations during the dehydration phase (Nordhoff and Ulrich 1999). This property can be explained by the lower solubility of trehalose in pure ethanol (close to 0) than in water (0.509 g/g solution) (Bouchard et al. 2007). Assuming that the initial dihydrate crystals are squares with a diameter of 800 μm, the specific surface area increases by a factor of more than 150 if these squares are transferred into a number of smaller anhydrates crystals of

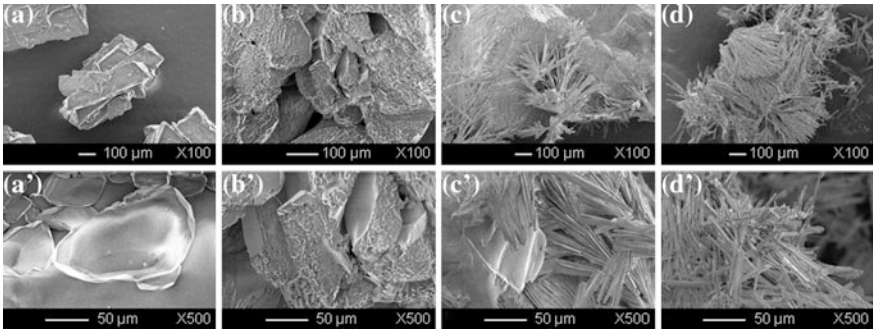

Fig. 8.6 Evolution of crystal structure through the isothermal crystal transformation at 70 °C using ethanol with 0.005 % water content. **a**, **a′** initial dihydrate trehalose; **b**, **b′** 20 min after reaction; **c**, **c′** 25 min after reaction; **d**, **d′** anhydrous trehalose obtained 30 min after reaction. The microscopy was performed at ×100 (**a**–**d**) and ×500 magnification (**a′**–**d′**)

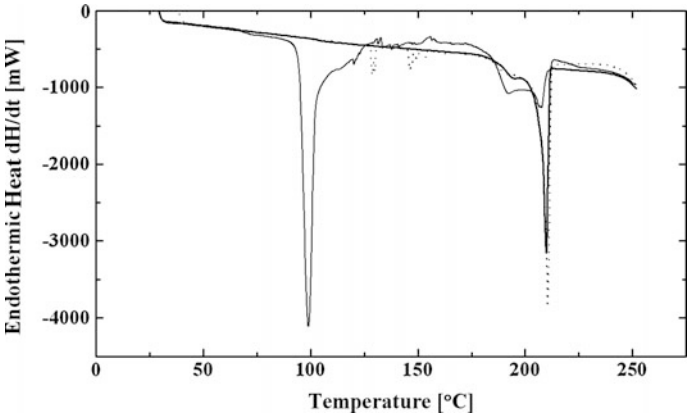

Fig. 8.7 Typical DSC thermographs of dihydrate trehalose (*thin line*), anhydrous trehalose obtained under isothermal (*thick line*) and non-isothermal conditions (*dashed line*)

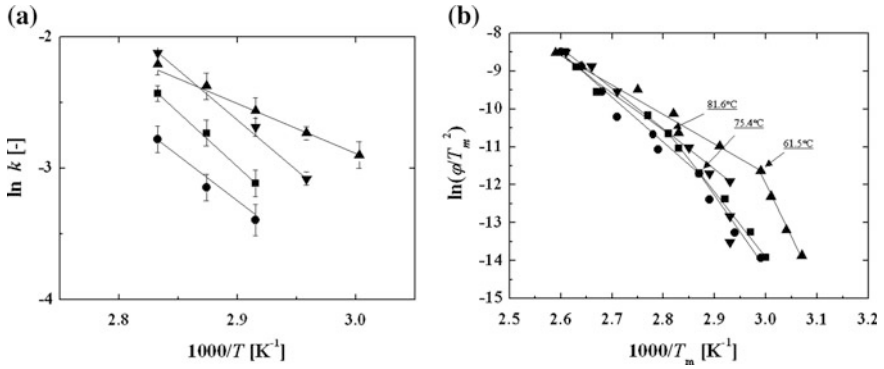

Fig. 8.8 Effect of the water content of ethanol on the crystal transformation kinetics under the **a** isothermal and **b** non-isothermal conditions (Kissinger's method). The water content of ethanol was 0.005 (*filled square*), 0.4 (*filled circle*), 2.5 (*upward pointing filled triangle*), and 4.0 % (*downward pointing filled triangle*)

100 μm in length and 3 μm in diameter. The increase in specific surface area is stronger if the diameter of the needle-like crystals is thinner.

Figure 8.7 shows the comparison between the DSC curves for the dihydrate and anhydrous trehalose. The dotted line represents the DSC curve of the anhydrous trehalose obtained under non-isothermal condition. The thermograph of the dihydrate trehalose revealed two peaks: a comparatively sharp peak at 100 °C, and a wider peak around 200 °C. The area of the endothermic peak of crystal transformation was approximated by numerical integration using Simpson's rule. The great number of data points makes this approximation highly accurate.

The crystallization kinetics of trehalose can be analyzed by the Avrami equation with 10 for the n parameter and the value of k which gave the best to the experimental data was calculated.

Table 8.2 Various properties of different β-maltose samples

Properties sample	Purity	β-form (%)	Degree of crystallinity (%)	DSC peak temperature (°C)	Crystallinity-corrected heat of fusion (J/g-crystal)
As-received Mβ-H_2O	99.3	96	91.0	131.6	191
$M\beta_s$	99.3	95	89.0	165.5	120
$M\beta_h$	99.3	93	84.8	132.4	73

$M\beta_s$ was obtained by ethanol-mediated transformation at 70 °C for 60 min, and $M\beta_h$ was obtained by vacuum drying at 56 °C for 4 days

Arrhenius plots of the transformation reaction rate constant, *k,* obtained under isothermal conditions are shown in Fig. 8.8. All displayed results correspond to an *n* value of 10. The activation energies of the crystal transformation E_i in ethanol of 0.005, 0.4, 2.5, and 4.0 % water content were determined to be 69, 62, 34, and 62 kJ/mol, respectively (Table 8.2). The activation energy at 2.5 % water content was only about half of that of the other treatments. In ethanol of 4.0 % water content, dehydration did not occur at temperatures below 65 °C.

The crystal transformation of dihydrate trehalose to anhydrous trehalose might be made up of two steps, which are crystal transformation from dihydrate trehalose to amorphous trehalose including the dehydration step and crystal growth from amorphous trehalose to anhydrous trehalose. The driving force of dehydration might be due to the higher chemical potential of water in the trehalose crystals.

We suppose that, for low temperature processes, the main phenomenon would be a diffusion of water of hydration of trehalose to the ethanol, increasing its water content. Moreover, the driving force of dehydration might be dependent on the water content in ethanol, and the diffusion coefficient of water in dihydrate trehalose might depend on the physical phase state of trehalose such as glassy state or rubbery state. Thus, the dehydration does not happen at low temperatures (glassy state) with 4.0 % water content in ethanol (lower driving force). The crystal growth rate might depend on the trehalose solubility in ethanol containing water. The increase in ethanol fraction causes a decrease in solubility of the dihydrate trehalose, has already been reported (Bouchard et al. 2007). Therefore, the water content of ethanol is the most important factor on this crystal transformation and affected the complex dependency of the crystal transformation rate.

8.7 Maltose

Maltose is arguably one of the most important sugars used in the food industry (Hodge et al. 1972, Odaka 1989). It is a disaccharide formed from two units of glucose joined with an α(1 → 4) bond. It is found in germinating seeds such as barley as they break down their starch to use for growth. Anhydrous maltose and maltose monohydrate are commercialized worldwide mostly as 90 % pure

crystalline product for the food industry. In addition, maltose is used in pharmaceuticals as a raw material, for example, in infusions in which it is sold as 99 % purity or above as a crystalline product. There are two anomers for maltose crystals: the α- and the β-forms, which have different crystal structures, melting points, solubility, and dissolution rates. In solution, one anomer can be converted into another by rearrangement of the position of the OH group in the open chain (anomerization). Maltose has three crystalline forms: anhydrous α-maltose (Quiqley et al. 1970), β-maltose monohydrate (Takusagawa and Jacobson 1978), and anhydrous β-maltose. Although they are anomers related via mutarotation, these forms can be regarded as polymorphs since there is a rapid inter-conversion between forms within solution. It is well recognized now that polymorphs, due to the difference in their potential energy levels, can have significant impact on the pharmaceutical behavior of a compound, for example, stability, solubility, and bioavailability.

In this study, the as-received maltose monohydrate (Mβ-H_2O) crystals were dehydrated using ethanol, and a new stable anhydrous β-maltose crystal form ($M\beta_s$) with fine pores was obtained. X-ray diffraction was used to characterize the crystalline difference from the anhydrous β-maltose obtained by vacuum drying ($M\beta_h$). In order to elucidate the reaction mechanism of the overall crystal transformation, the evolution of water content in the sample was measured. Thermal analysis was performed and the reaction kinetics was analyzed by the Jander and the Arrhenius equations. The evolution of the surface structure and anomer ratio was also investigated using scanning electron microscopy and gas chromatography.

The evolution of the crystal structure during crystal transformation at 50 °C is shown in Fig. 8.9. Before the reaction started, the as-received Mβ-H_2O crystals were present in a variety of shapes with sizes ranging from 100 to 300 μm and smooth surfaces. After 10 min of reaction time, some small pores were formed at the surface of the initial crystals. The number of pores increased as the reaction progressed. After 60 min of reaction, the crystal surface was covered with numerous needle-like crystals with a diameter below 1 μm and a maximum length of 10 μm. The crystal surface looked similar after 180 min of reaction and did not

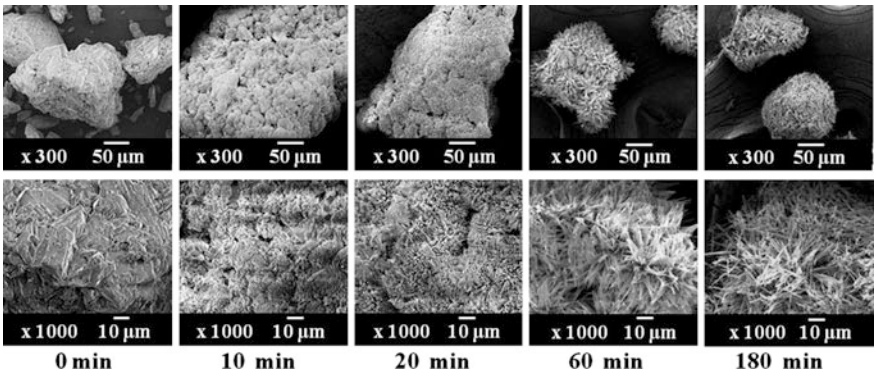

Fig. 8.9 Evolution of maltose crystal structure during crystal transformation in ethanol at 50 °C

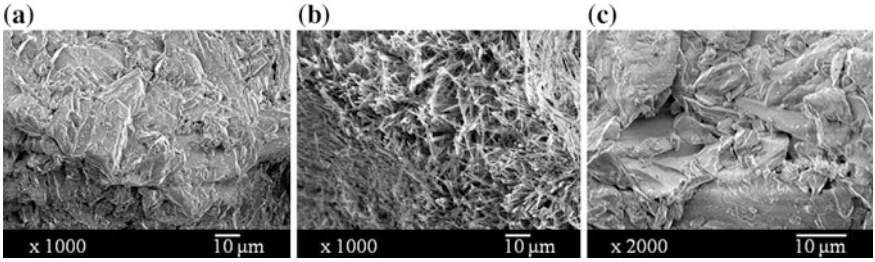

Fig. 8.10 Morphological comparison of **a** the as-received Mβ-H_2O, **b** $M\beta_s$, and **c** $M\beta_h$ crystals

seem to evolve more. The surface structures of three kinds of maltose crystals, the as-received Mβ-H_2O, $M\beta_s$, and $M\beta_h$ are shown in Fig. 8.10. $M\beta_s$ particles appeared to be porous aggregations of fine needle-like crystals. In contrast to $M\beta_s$, the as-received Mβ-H_2O and $M\beta_h$ both presented smooth surfaces.

The specific surface area of the porous $M\beta_s$, measured by the nitrogen adsorption isotherms, was 3.39 m^2/g, and those of the as-received Mβ-H_2O and $M\beta_h$ were 0.46 and 0.82 m^2/g, respectively. The specific surface area of $M\beta_s$ was about four- to sevenfold larger than those of the as-received Mβ-H_2O and $M\beta_h$. $M\beta_s$ also showed a relatively large intrusion volume (1.05 mL/g) and a median pore diameter of 1.26 µm, as measured by the mercury filling method (Ohashi 2010). The as-received Mβ-H_2O and $M\beta_h$ had much larger median pore diameters of 11.2 and 14.7 µm, respectively.

DSC profiles of the as-received Mβ-H_2O, $M\beta_s$, and $M\beta_h$ are illustrated in Fig. 8.11. $M\beta_s$ used was obtained by ethanol-mediated transformation at 70 °C for 60 min, and $M\beta_h$ was obtained by vacuum drying at 56 °C for 4 days. The as-received Mβ-H_2O presented a single endothermic peak at 131.6 °C (a), while $M\beta_h$ showed a unique peak at 132.4 °C (c). Although $M\beta_h$ is anhydrous, the similarity in melting point between these two crystalline forms revealed that $M\beta_h$ was actually metastable and would tend

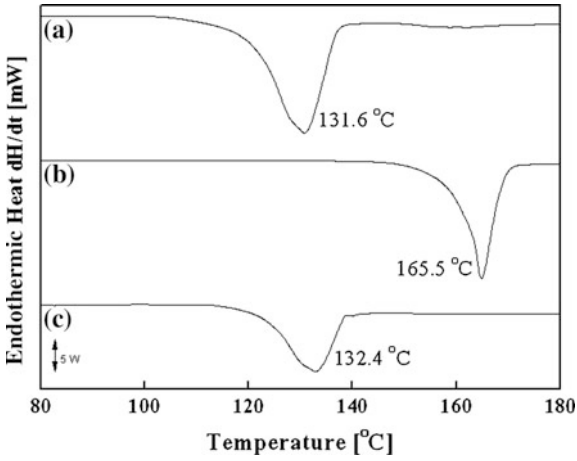

Fig. 8.11 Typical DSC profiles of **a** the as-received Mβ-H_2O, **b** $M\beta_s$, and **c** $M\beta_h$

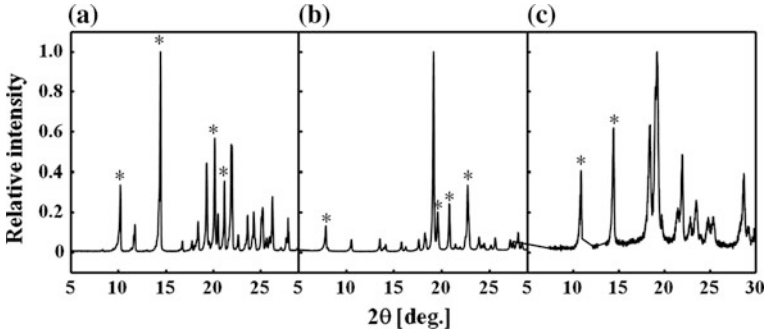

Fig. 8.12 Powder X-ray diffraction patterns of **a** the as-received Mβ-H_2O, **b** $M\beta_s$, and **c** $M\beta_h$. The symbol "*asterisk*" denotes a specific diffraction peak

to adsorb water to switch back to Mβ-H_2O. On the contrary, $M\beta_s$ (b) had a single peak at a much higher temperature (165.5 °C), which may be a clue of a higher stability. The as-received Mβ-H_2O crystals were of ca. 99.3 % purity, and the pure Mβ-H_2O was present mostly in the crystalline state (ca. 91 %), with a small fraction existing in the non-crystalline form (ca. 8.3 %). Table 8.1 shows the crystallinity-corrected heat of fusion of the three types of β-maltose crystals: the as-received Mβ-H_2O, $M\beta_s$, and $M\beta_h$. The uncorrected heat of fusion of the as-received Mβ-H_2O and $M\beta_s$ measured by DSC were 174 and 107 J/g of sample, respectively. The crystallinity-corrected heat of fusion of the β-form crystals were 191 and 120 J/g-crystal, respectively.

Powder X-ray diffraction of the as-received Mβ-H_2O (a), $M\beta_s$ (b), and $M\beta_h$ (c) are shown in Fig. 8.12. The as-received Mβ-H_2O showed characteristic diffraction peaks at 10.2°, 14.4°, 20.1°, and 21.2°. $M\beta_s$ had specific diffraction peaks at 7.9°, 19.2°, 20.8°, and 22.7°. $M\beta_h$ showed specific diffraction peaks at 10.9° and 14.8°. The results confirmed that $M\beta_s$ and $M\beta_h$ had completely different crystal forms. Kirk et al. (2007) and Crisp et al. (2010) have reported that the same characteristic powder X-ray diffraction pattern was generated from $L\alpha_s$ samples created by the dehydration of Lα-H_2O using both thermal (hard method) and solvent-mediated methods (soft method), indicating the same crystalline structure in both cases. Nonetheless, $M\beta_s$ was not obtainable by thermal treatment, but only via ethanol-mediated crystal transformation. The stable form of anhydrous β-maltose, $M\beta_s$ prepared in this paper would be advantageous for applications in the food and pharmaceutical industries, where thermodynamically stable crystalline forms are preferred for improvement of the shelf stability of products.

Figure 8.13 shows the time course of the moisture content of the maltose samples at different reaction temperatures (45, 50, 55, 60, and 70 °C). Dehydration is part of the crystal transformation process from Mβ-H_2O to anhydrous maltose. The solid lines are obtained by fitting Jander's equation to the experimental results. These good correlations suggested that the diffusion of water in maltose might be the rate-limiting process of this crystal transformation. The initial moisture content of the as-received Mβ-H_2O was 5.0 ± 0.1 %. The dehydration reaction was faster at higher temperatures. For 60 and 70 °C, the moisture content dropped to 0.5 %

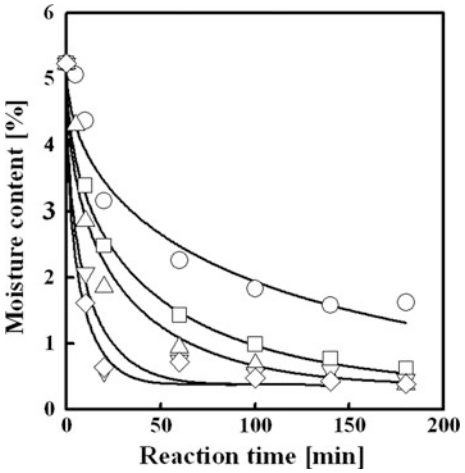

Fig. 8.13 Time courses of moisture content of β-maltose during ethanol-mediated crystal transformation at: 45 °C (*circle*), 50 °C (*square*), 55 °C (*upward pointing triangle*), 60 °C (*downward pointing triangle*), and 70 °C (*diamond*)

after 60 min of reaction. For 55 and 50 °C, the moisture content also decreased to 0.5 %, but a longer reaction time was needed (about 180 min). For the dehydration process at 45 °C, the dehydration reaction speed was the lowest, reaching a value of 1.6 % moisture content after 180 min and needed about 500 min to be completed. A minimum temperature of 50 °C was suitable to accomplish a complete transformation from Mβ-H_2O to $M\beta_s$ within 200 min.

In order to calculate the crystal conversion by the heat of fusion, the heat of fusion of both Mβ-H_2O and its dehydrated crystal, $M\beta_s$, are necessary to know. Figure 8.14 shows the time courses of the conversions determined by the disappearance of Mβ-H_2O (left) and the formation of $M\beta_s$ (right) with time at several temperatures. The conversions were calculated using the heat of fusion obtained by DSC measurements. Likewise, the solid lines are obtained by fitting Jander's equation to the empirical results. Modeling the conversion profiles using Jander's equation was satisfactory. The disappearance of Mβ-H_2O was roughly compensated by the formation of $M\beta_s$, indicating the conversion of Mβ-H_2O to $M\beta_s$. The apparent conversion rate constant increased with the increase in temperature. Mutarotation did not sufficiently occur during the crystal transformation of maltose by ethanol, as shown in Table 8.1. The as-received Mβ-H_2O contained 96 % β-form, and $M\beta_s$ contained 95 % β-form. This value is close to that obtained by Hodge et al. (1972) for $M\beta_h$ (93 % β-form). However, when placed in an environment at 57 % relative humidity (RH), the water content of $M\beta_h$ increased to 5.0 % after 2 h (initially 0.5 %), while $M\beta_s$ had a water content of 1.0 % after 100 h of storage at 57 % RH. $M\beta_s$ could presumably be considered a stable form of anhydrous β-maltose.

Jander's equation was also applied to the water loss in Mβ-H_2O to obtain the Arrhenius plots as illustrated in Fig. 8.15. The activation energy for the dehydration of Mβ-H_2O was found to be 100 kJ/mol, while the activation energy for the formation of $M\beta_s$ was 90 kJ/mol. The mechanism of the crystal transformation may consist of two steps. The first step would be the dehydration of Mβ-H_2O by ethanol and the dissolution to the amorphous state, which happened comparatively quite rapidly for higher

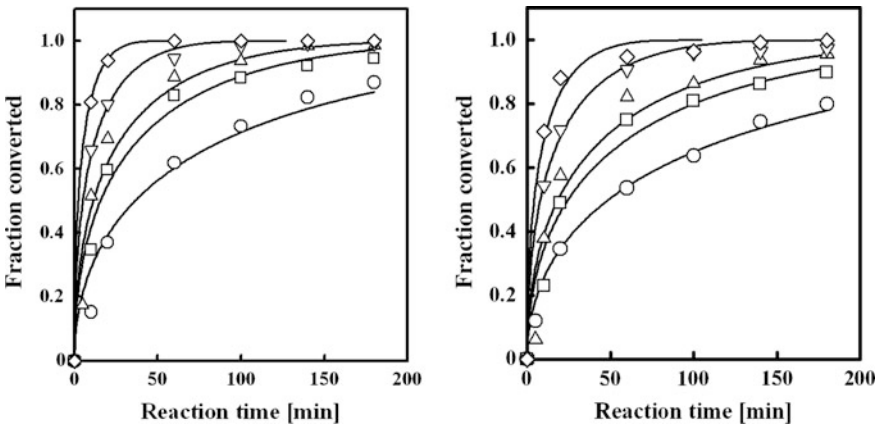

Fig. 8.14 Time courses of the conversions determined by the disappearance of Mβ-H_2O (*left*) and the formation of $M\beta_s$ (*right*) in ethanol at several temperatures. *Circle* 45 °C, *square* 50 °C, *upward pointing triangle* 55 °C, *downward pointing triangle* 60 °C, and *diamond* 70 °C. The *symbols* represent the calculated heats of fusion obtained by DSC measurements. The *solid lines* are the fittings of the empirical data by Jander's equation

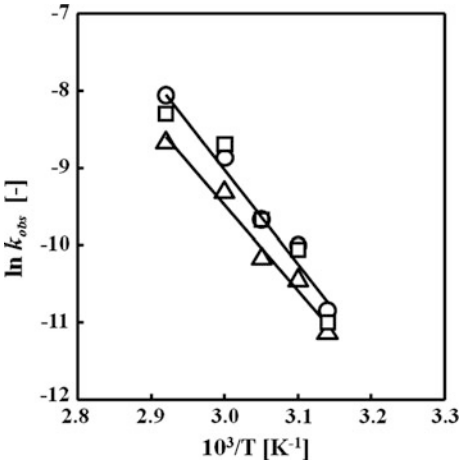

Fig. 8.15 Arrhenius plots of the conversion rates determined by the water loss in Mβ-H_2O (*circle*), the disappearance of Mβ-H_2O (DSC) (*square*), and the formation of $M\beta_s$ (DSC) (*diamond*)

temperatures. The second step would be the nucleation of $M\beta_s$ on the surface and its subsequent growth. This idea is confirmed by the variation of the conversion rates observed for a reaction carried out at 50 °C (Fig. 8.16). From this figure, it is understood that the conversion rate of the three reactions evolved the same way. However, the formation of $M\beta_s$ was not instant and seemed to proceed with a slight delay. This small lap of time would be necessary for the transition from the amorphous phase to the anhydrous crystalline form. The difference between the solubility of Mβ-H_2O (relatively high in ethanol containing a small amount of water) (Bouchard et al. 2007) and $M\beta_s$ drives the dissolution process and consequently determines the supersaturation

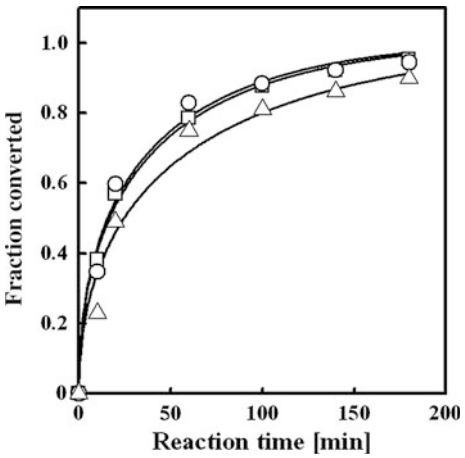

Fig. 8.16 Comparison of the conversions observed during the crystal transformation process carried out at 50 °C. The plots are the experimental data and the *solid lines* show the fittings of empirical data by Jander's equation. Water loss in the as-received Mβ-H_2O (*circle*). Disappearance of Mβ-H_2O (DSC) (*square*). Formation of $M\beta_s$ (DSC) (*diamond*)

level during the crystallization of $M\beta_s$. The ethanol-mediated crystal transformation of maltose might be dissolution controlled for lower temperatures, and crystallization controlled for higher temperatures, as indicated by the different activation energies for the dehydration and crystallization. Zhu et al. (1996) pointed out that in an anhydrate/hydrate system in mixtures of water and an organic solvent, water activity plays a crucial role. For a given temperature, there is an equilibrium value of water activity at which the solubility of the hydrate and the anhydrate are equal. The phase transformation from Mβ-H_2O to $M\beta_s$ may be the consequence of a deviation from the equilibrium water activity. The moisture content of ethanol is, therefore, a very important parameter of the crystal transformation. Anomerization of maltose is likely to happen in anhydrous polar solvents such as ethanol. Garnier et al. (2002) observed that the use of acetone as dehydrating solvent on single crystals of Lα-H_2O, without stirring, led to the unexpected formation of single crystals of the anomeric β-lactose (Lβ). The phenomenon was attributed to a complex mechanism, which requires minimum diffusion, so that mutarotation can occur before diffusion of water in acetone. Hence, Lβ was not obtained from a stirred suspension of Lα-H_2O in acetone. In ethanol, $L\alpha_s$ could be obtained from Lα-H_2O, probably via nucleation and growth processes. Since the solubility of $L\alpha_s$ is very low in ethanol (Bouchard et al. 2007), mutarotation would be unlikely in this solvent at room temperature. In the present ethanol-mediated crystal transformation of maltose, constant agitation assured sufficient diffusion preventing mutarotation at temperatures above 50 °C. As the reaction progressed, the moisture content of ethanol increased. This might be responsible for the reduction of $M\beta_s$ nucleation and growth rates because of the increasing supersaturation ratio.

Encapsulation of flax seed oil in crystalline maltose and trehalose with porous and non-porous structures was investigated to improve the stability of fatty acid during storage in the encapsulated oil (Ohashi et al. 2008). Anhydrous crystalline maltose and trehalose with a fine porous structure were obtained by dehydration using ethanol. The oil powders encapsulated with anhydrous crystalline maltose and trehalose with porous structure had good fluidity. The stability of fatty acids in

the encapsulated oil powders was investigated for storage at 40 °C. By using crystalline trehalose to encapsulate the fatty acids, degradation was markedly inhibited, irrespective of structure porosity. Formation of volatile aldehydes in porous crystalline trehalose or maltose was reduced to about half the amount of that for the non-porous crystalline encapsulates, indicating that volatile aldehyde was adsorbed into the fine pores.

8.8 Conclusion

In this chapter, the kinetics and mechanism of crystal transformation were discussed, as well as the influence on the crystal structure and the possible applications. The target compounds were mainly carbohydrates, including trehalose and maltose. Ethanol-mediated crystal transformation of sugars can lead to the formation of anhydrous porous crystal material with high specific surface area. These newly obtained sugar crystals have specific properties to form a creamy gel of sugar at supersaturated concentration. We can apply this porous sugar crystal to encapsulate flavor or functional food for the delivery of those compounds with release rate control.

References

Aguilar CA, Hollender R, Ziegler GR (1994) Sensory characteristics of milk chocolate with lactose from spray-dried milk powder. J Food Sci 59(6):1239–1243

Akao K, Okubo Y, Asakawa N, Inoue Y, Sakurai M (2001) Infrared spectroscopic study on the properties of the anhydrous form II of trehalose. Implications for the functional mechanism of trehalose as a biostabilizer. Carb Res 334:233–241

Alie J, Menegotto J, Cardon P, Duplaa H, Caron A, Lacabanne C, Bauer M (2004) Dielectric study of the molecular mobility and the isothermal crystallization kinetics of amorphous pharmaceutical drug substance. J Pharm Sci 93(1):218–233

Arvanitoyanis I, Blanshard J (1994) Rates of crystallization of dried lactose-sucrose mixtures. J Food Sci 59(1):197–205

Avrami M (1939) Kinetics of phase change I. J Chem Phys 7:1103–1112

Avrami M (1940) Kinetics of phase change II. J Chem Phys 8:212–224

Beckett ST, Francesconi MG, Geary PM, Mackenzie G, Maulny APE (2006) DSC study of sucrose melting. Carb Res 341:2591–2599

Boode K, Bisperink C, Walstra P (1991) Destabilization of O/W emulsions containing fat crystals by temperature cycling. Colloids Surf 61:55–74

Bouchard A, Hofland GW, Witkamp GJ (2007) Properties of sugar, polyol, and polysaccharide water-ethanol solutions. J Chem Eng Data 52:1838–1842

Buckton G, Chidavaenzi OC, Koosha F (2002) The effect of spray-drying feed temperature and subsequent crystallization conditions on the physical form of lactose. AAPS Pharm Sci Tech 3(4): Technical note 1

Cal S, Rodríguez-Puente B, Souto C, Concheiro A, Gómez-Amoza JL, Martínez-Pacheco R (1996) Comparison of a spray-dried α-lactose monohydrate with a fully hydrated roller-dried β-lactose. Int J Pharm 136:13–21

Carstensen T, Van Scoik K (1990) Amorphous-to-crystalline transformation of sucrose. Pharm Res 7:1278–1281

Chidavaenzi OC, Buckton G, Koosha F, Pathak R (1997) The use of thermal techniques to assess the impact of feed concentration on the amorphous content and polymorphic forms present in spray dried lactose. Int J Pharm 159:67–74

Christensen KL, Pedersen GP, Kristensen HG (2002) Physical stability of redispersible dry emulsions containing amorphous sucrose. Eur J Pharm Biopharm 53:147–153

Crisp JL, Dann SE, Edgar M, Blatchford CG (2010) The effect of particle size on the dehydration/rehydration behaviour of lactose. Int J Pharm 391:38–47

Crowe JH (1971) Anhydrobiosis: an unsolved problem. Am Nat 105:563–573

Crowe LM, Reid DS, Crowe JH (1996) Is trehalose special for preserving dry biomaterials? Biophys J 71:2087–2093

Devlin TM (ed) (2002) Amino acid metabolism, chapter no 18 of textbook of biochemistry with clinical correlations, 5th edn, pp 784–790. Wiley-Liss, New York

Figura LO, Epple MJ (1995) Anhydrous α-lactose. A study with DSC and TXRD. J Thermal Anal 44:45–53

Furuki T, Abe R, Kawaji H, Atake K, Sakurai M (2006) Thermodynamic functions of α, α-trehalose dihydrate and of α, β-trehalose monohydrate at temperatures from 13 K to 300 K. J Chem Thermodyn 38:1612–1619

Garnier S, Petit S, Coquerel G (2002) Dehydration mechanism and crystallinsation behaviour of lactose. J Therm Anal Cal 68:489–502

Gloria H, Sievert D (2001) Changes in the physical state of sucrose during dark chocolate processing. J Agric Food Chem 49:2433–2436

Grön H, Borissova A, Roberts KJ (2003a) In-process ATR-FTIR spectroscopy for closed-loop supersaturation control of a batch crystallizer producing monosodium glutamate crystals of defined size. Ind Eng Chem Res 42:198–206

Grön H, Mougin P, Thomas A, White G, Wilkinson D (2003b) Dynamic in-process examination of particle size and crystallographic form under defined conditions of reactant supersaturation as associated with the batch crystallization of monosodium glutamate from aqueous solution. Ind Eng Chem Res 42:4888–4898

Gabarra P, Hartel W (1998) Corn syrup solids and their saccharide fractions affect crystallization of amorphous sucrose. J Food Sci 63:523–528

Hammond RB, Lai X, Roberts KJ, Thomas A, White G (2004) Application of in-process X-ray powder diffraction for the identification of polymorphic forms during batch crystallisation reactions. Cryst Growth Design 4:943–948

Hancock JD, Sharp JH (1972) Method of comparing solid-state kinetic data and its application to the decomposition of kaolinite, brucite, and $BaCO_3$. J Am Cera Soc 55:74–77

Hartel Ri W, Shastry AV (1991) Sugar crystallization in food products. Crit Rev Food sci Nutr 30(1):49–112

Higashiyama T (2002) Novel functions and applications of trehalose. Pure Appl Chem 74 (7):1263–1269

Hodge JE, Rendleman JA, Nelson EC (1972) Useful properties of maltose. Cereal Sci Today 17:180–188

Hulbert SF (1969) Models for solid state reactions in powdered compacts. J Br Ceram Soc 6:11–20

Hurtta M, Pitkanen I, Knuutinen J (2004) Melting behaviour of D-sucrose, D-glucose and D-fructose. Carb Res 339:2267–2273

Jander WZ (1927) Reactions in the solid state at high temperatures I. Rate of reaction for an endothermic change. Anorg U Allgem Chem 163:1–30

Jones MD, Beezer AE, Buckton G (2008) Determination of outer layer and bulk dehydration kinetics of trehalose dihydrate using atomic force microscopy, gravimetric vapour sorption and near infrared spectroscopy. J Pharm Sci 97:4404–4415

Jones MD, Hooton JC, Dawson ML, Ferrie AR, Price R (2006) Dehydration of trehalose dihydrate at low relative humidity and ambient temperature. Int J Pharm 313:87–98

Kedward CJ, Macnaughtan W, Blanshard JMV, Mitchell JR (1998) Crystallization kinetics of lactose and sucrose based on isothermal differential scanning calorimetry. J Food Sci 63(2):192–197

Kedward CJ, Macnaughtan W, Mitchell JR (2000) Crystallization kinetics of amorphous lactose as a function of moisture content using isothermal differential scanning calorimetry. J Food Sci 65 (2):324–328

Kilburn D, Sokol PE (2009) Structural evolution of the dihydrate to anhydrate crystalline transition of trehalose as measured by wide-angle X-ray scattering. J Phys Chem B 113:2201–2206

Kimmerling ZJ (1984) An attempt to investigate changes of impurity concentration with the depth of crystal matrix of VHP sugar. Proc Congr S Afr Sugar Technol Assoc 58:51–53

Kirk JH, Dann SE, Blatchford CG (2007) Lactose: a definitive guide to polymorph determination. Int J Pharm 334:103–114

Kissinger HE (1957) Reaction kinetics in differential thermal analysis. Anal Chem 29:1702–1706

Lappalainen M, Pitkänen I, Harjunen P (2006) Quantification of low levels of amorphous content in sucrose by hyperDSC. Int J Pharm 307:150–155

Maruyama S, Ooshima H (2001) Mechanism of the solvent-mediated transformation of taltirelin polymorphs promoted by methanol. Chem Eng J 81:1–7

Mathlouthi M, Cholli AL, Koenig JL (1986) Spectroscopic study of the structure of sucrose in the amorphous state and in aqueous solution. Carb Res 147:1–9

Mazzobre MF, Soto G, Aguilera JM, Buera MP (2001) Crystallization kinetics of lactose in sytems co-lyofilized with trehalose. Analysis by differential scanning calorimetry. Food Res Int 34:903–911

Nagase H, Endo T, Ueda H, Nagai T (2003) Influence of dry conditions on dehydration of α, α-trehalose dihydrate. STP Pharma Sci. 13:269–275

Nakai Y, Yamamoto K, Terada K, Sasaki I (1986) Crystallization of amorphous α-, β-, γ-cyclodextrin by water sorption. Yakugaku Zasshi 106:420–424

Nordhoff S, Ulrich J (1999) Solvent-induced phase transformations of hydrates. J Therm Anal Cal 57:181–192

O'Brien J (1996) Stability of trehalose, sucrose and glucose to nonenzymatic browning in model systems. J Food Sci 61:679–682

Odaka E (1989) Anhydrous maltose. New Food Indus (in japanese) 17–22

Ohashi T (2010) Porous crystalline saccharide, its preparation and uses. U.S. patent 0222569 A1

Ohashi T, Yoshii H, Furuta T (2007) Innovative crystal transformation of dihydrate trehalose to anhydrous trehalose using ethanol. Carb Res 342:819–825

Ohashi T, Shibuya T, Oku K, Yoshii H, Furuta T (2008) Encapsulation of flax seed oil in anhydrous crystalline maltose and trehalose with porous structure (in Japanese). Nippon Shokuhin Kagaku Kogaku Kaishi. 55(1):13–17

Ohashi T, Verhoeven N, Okuda D, Furuta T, Yoshii H (2009) Formation of porous α-CD ethanol dihydrate by crystal transformation method. Eur Food Res Technol 230:195–199

Okuno M, Kishihara S, Otsuka M, Fujii S, Kawasaki K (2003) Variability of melting behavior of commercial granulated sugar measured by differential scanning calorimetry. Int Sugar J 105:29–35

Orford PD, Paker R, Ring SG (1990) Aspects of the glass transition behaviour of mixtures of carbohydrates of low molecular weight. Carb Res 196:11–18

Parrish MW, Brown ML (1982) Solid state transformations of α-Lactose monohydrate in alcoholic media. J Dairy Sci 65:1688–1691

Peica N, Lehene C, Leopold N, Schlucker S, Kiefer W (2007) Monosodium glutamate in its anhydrous and monohydrate form: differentiation by Raman spectroscopies and density functional calculations. Spectrochim Acta Part A 66:604–615

Pinto SS, Diogo HP, Moura-Ramos JJ (2006) Crystalline anhydrous α,α-trehalose (polymorph β) and crystalline dihydrate α,α-trehalose: a calorimetric study. J Chem Thermodyn 38: 1130–1138

Pitchayajittipong C, Price R, Shur J, Kaerger JS, Edge S (2010) Characterisation and functionality of inhalation anhydrous lactose. Int J Pharm 390:134–141

Quigley GJ, Sarko A, Marchessault RH (1970) Crystal and molecular structure of maltose monohydrate. J Am Chem Soc 92(20):5834–5839

Reisener HJ, Goldschmid HR, Ledingham GA, Perlin AS (1962) Formation of trehalose and polyols by wheat stem rust (*Puccinia graminis tritici*) uredospores. Can J Biochem Physiol 40:1248–1251

Rousseau D (2000) Fat crystals and emulsion stability—a review. Food Res Int 33(1):3–14

Roos Y, Karel M (1992) Crystallization of amorphous lactose. J Food Sci 57:775–777

Roos Y (1993) Melting and glass transitions of low molecular weight carbohydrates. Carb Res 238:39–48

Saleki-Gerhardt A, Zografi G (1994) Non-isothermal and isothermal crystallization of sucrose from the amorphous state. Pharm Res 11(8):1166–1173

Simperler A, Kornherr A, Chopra R, Bonnet PA, Jones W, Motherwell WDS, Zifferer G (2006) Glass transition temperature of glucose, sucrose, and trehalose: An experimental and in silico study. J Phys Chem B 110:19678–19684

Sola-Penna M, Meyer-Fernandes JR (1998) Stabilization against thermal inactivation promoted by sugars on enzyme structure and function: why is trehalose more effective than other sugars? Arch Biochem Biophys 360(1):10–14

Stryer L (ed) (1988). Biochemistry, 3rd edn, pp 18, 496, 579, 1026, Freeman, W.H, New York

Supratim G, Rousseau D (2011) Fat crystals and water-in-oil emulsion stability. Curr Opin Coll 16(5):421–431

Surana R, Pyne A, Suryanarayanan R (2004) Effect of preparation method on physical properties of amorphous trehalose. Pharm Res 21(7):1167–1176

Sussich F, Bortoluzzi S, Cesàro A (2002) Trehalose dehydration under confined conditions. Therm Acta 391:137–150

Sussich F, Cesàro A (2008) Trehalose amorphization and recrystallization. Carb Res 343:2667–2674

Sussich F, Skopec CE, Brady JW, Cesàro A (2001) Reversible dehydration of trehalose and anhydrobiosis: from solution state to an exotic crystal? Carbohydr Res 334:165–176

Sussich F, Skopec CE, Brady JW, Cesàro A (2010) Water mobility in the dehydration of crystalline trehalose. Food Chem 122:388–393

Sussich F, Urbani R, Princivalle F, Cesàro A (1998) Polymorphic amorphous and crystalline forms of trehalose. J Am Chem Soc 120:7893–7899

Takusagawa F, Jacobson RA (1978) The crystal and molecular structure of α-maltose. Acta Cryst B 34:213–218

Teramoto N, Sachinvala ND, Shibata M (2008) Trehalose and trehalose-based polymers for environmentally benign, biocompatible and bioactive materials. Molecules 13:1773–1816

Threlfall T (1995) Analysis of organic polymorphs. A review. Analyst 120:2435–2460

Urbani R, Sussich F, Prejac S, Cesaro A (1997) Enthalpy relaxation and glass transition behaviour of sucrose by static and dynamic DSC. Therm Acta 304(305):359–367

Vanhal I, Blond G (1999) Impact of melting conditions of sucrose on its glass transition temperature. J Agri Food Chem 47:4285–4290

Van Scoik KG, Carstensen JT (1990) Nucleation phenomena in amorphous sucrose systems. Int J Pharm 58:185–196

Vromans H, Bolhuis GK, Lerk CF, Kus-sendrager KD (1987) Studies on tableting properties of lactose VIII. The effect of variations in primary particle size, percentage of amorphous lactose and addition of a disintegrant on the disintegration of spray-dried lactose tablets. Int J Pharm 39:201–206

Weibull W (1951) A statistical distribution function of wide applicability. J Appl Mech 18:293–297

Willart JF, Danede F, De Gusseme A, Descamps M, Neves C (2003) Origin of the dual structural transformation of trehalose dihydrate upon dehydration. J Phys Chem B 107:11158–11162

Zhu H, Yuen C, Grant DJW (1996) Influence of water activity in organic solvent + water mixtures on the nature of the crystallizing drug phase. I Theophylline Int J Pharm 135:151–160